The performance of organic electronic ratchets

The performance of organic electronic ratchets

Erik M. Roeling,[1] Wijnand Chr. Germs,[1] Barry Smalbrugge,[2] Erik Jan Geluk,[2] Tjibbe de Vries,[2] René A. J. Janssen,[1] and Martijn Kemerink[1,a]
[1]*Applied Physics, Eindhoven University of Technology, PO Box 513, Eindhoven, the Netherlands*
[2]*COBRA Research Institute, Eindhoven University of Technology, PO Box 513, Eindhoven, the Netherlands*

(Received 21 October 2011; accepted 26 December 2011; published online 10 January 2012)

Organic electronic ratchets rectify time-correlated external driving forces, giving output powers that can drive electronic circuitry. In this work their performance characteristics are investigated using numerical modeling and measurements. It is shown how the characteristic parameters of the time–varying asymmetric potential like length scales and amplitude, as well as the density and mobility of the charge carriers in the device influence the performance characteristics. Various ratchet efficiencies and their relations are discussed. With all settings close to optimum, a ratchet with charge displacement and power efficiencies close to 50% and 7% respectively is obtained. [doi:10.1063/1.3677934]

I. INTRODUCTION

Ratchets have been known for over a century as complex, counterintuitive devices. Originally they were conceived by Smoluchowski and later Feynman to discuss the intricacies of thermodynamics.[1,2] Practical use of man-made ratchets has been relatively limited, with the main (proposed) use being the fractionation of particle distributions.[3] Electrically, the ratchet principle has mainly been used in (quantum) charge pumps.[4–6] In a recent publication we have introduced organic electronic ratchets that operate at room temperature and from which enough work can be extracted to drive simple logic circuitry.[7] Drift–diffusion simulations presented in Ref. 7 indicate that their power efficiency can be as high as 1.5%. Although it was shown that these ratchets yield their high output powers by the grace of charge-charge interactions, a more detailed understanding of the factors limiting their performance, and, concomitantly, a view on how and to which extent performance can be optimized is still lacking. In a broader perspective, the organic electronic ratchet is particularly suited for a performance study on ratchets in general because of its rich multi-dimensional parameter space in which geometrical, temporal and population parameters all are experimentally easily accessible. Ultimately, ratchets could be systems where control over the electrostatic potential on the nanoscale is employed to efficiently scavenge energy from external sources.

In this work, the influence of system parameters like asymmetry, magnitude and frequency of the driving force on the performance characteristics of electronic ratchets is addressed; in particular the output characteristics, the power efficiency, and the charge displacement efficiency are studied. A two-dimensional drift–diffusion model is used to investigate the performance parameters. The model is calibrated by quantitative comparison to measurement results. It is found that the charge displacement and power efficiencies of an optimized device can be close to 50% and 7 % respectively; an intuitive relation between the two is found. The results suggest that ratchets, indeed, might be useful as compact energy scavengers.

[a]Author to whom correspondence should be addressed. Electronic mail: m.kemerink@tue.nl.

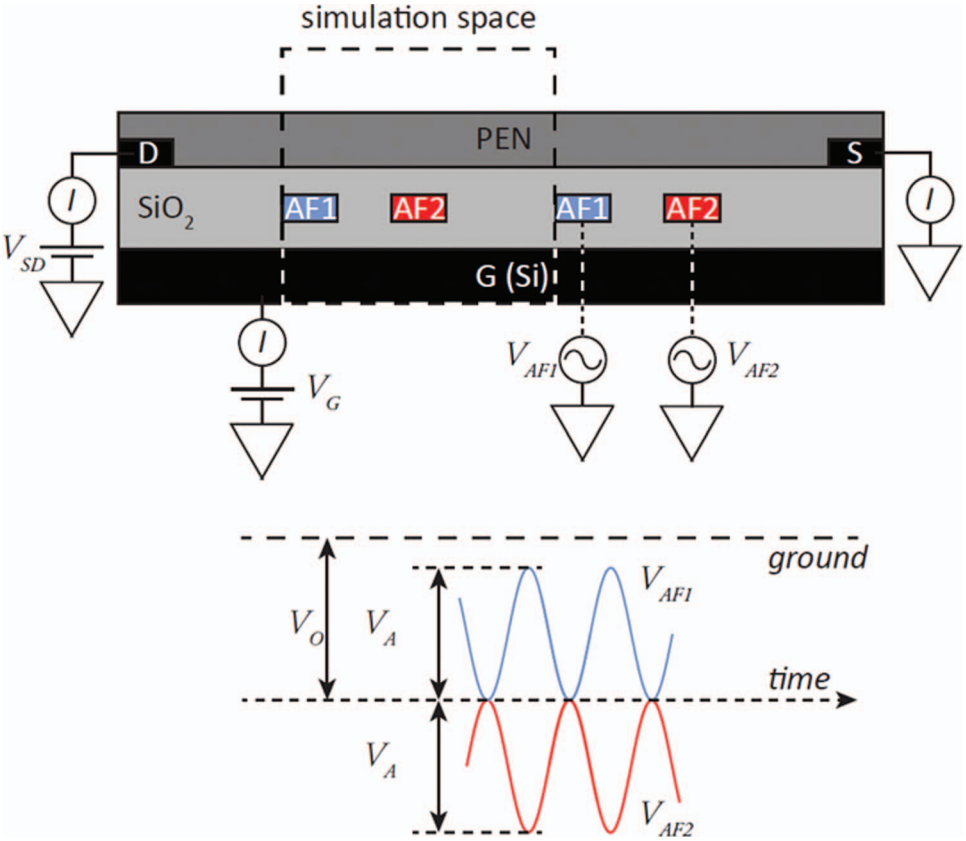

FIG. 1. Cross section of an L1–2P2 electronic ratchet. Visible are the source (S) and drain (D) contacts, which are separated from the silicon (Si) gate (G) contact by the silicon dioxide (SiO_2) gate dielectric. Asymmetrically spaced interdigitated finger electrodes denoted by AF1 and AF2 are placed inside the gate dielectric. Note the color coding of the finger electrodes; fingers with the same color are electrically connected. Pentacene (PEN) is used as a semiconductor. Note that the potentials V_{AF1} and V_{AF2} as a function of time are shown in anti–phase, which is not necessarily the case.

II. METHODS

This section introduces the layout and fabrication of the investigated ratchet devices and describes their operation along with some experimental details. Next, definitions of various ratchet efficiencies are given followed by a description of the numerical model employed in this work.

A. Device layout and measurements

In Figure 1(a) cross section of a typical organic electronic ratchet is shown. It is built around a conventional bottom-gate bottom-contact organic field effect transistor in which asymmetrically spaced interdigitated finger electrodes have been embedded in the SiO_2 gate dielectric. The ratchets were fabricated as described previously on Si wafers covered by 100 nm of thermal SiO_2.[7] Asymmetric interdigitated finger electrodes (5 nm Ti/20 nm Au/5 nm Ti, 1 μm wide, 1.5 mm long) are deposited by UV photolithography and lift-off. They are covered with 100 nm SiO_2 layer deposited by plasma enhanced chemical vapour deposition. Subsequently, two (10 nm Ti/40 nm Au, 1 mm long) contacts are positioned symmetrically with respect to the interdigitated fingers on top of the SiO_2 layer, again by UV photolithography and lift-off. A monolayer of hexamethyldisilazane (HMDS) is applied after which 50 nm pentacene is deposited by thermal evaporation.

Measurements are conducted at 40 °C in a high-vacuum probe station. Prior to the measurements the sample is in situ heated to 110 °C for over one hour to remove water. A Keithley 4200 parameter analyzer equipped with pre-amplifiers is used to source voltage and measure current at source, drain

and gate contacts. The source contact is kept at zero bias. An Agilent 81150 dual channel arbitrary waveform generator is used to apply the potentials on AF1 and AF2. The oscillating potentials applied to the finger electrodes are $V_{AF1}(t)=V_0+(V_A/2)(1+\sin(\omega t))$ and $V_{AF2}(t)=V_0-(V_A/2)(1+\sin(\omega t+\varphi))$. Here V_O is a central offset voltage, V_A is the amplitude of the ratchet potential (i.e. the peak–peak voltage of each individual potential), ω the angular frequency, t the time and φ the phase difference between V_{AF1} and V_{AF2}. Unless stated otherwise, the phase difference between V_{AF1} and V_{AF2} is always 180° (Figure 1); near the end of this manuscript the influence of the phase difference φ on current and charge transport is explicitly addressed.

B. Ratchet operation and notation

The operational principle of the present ratchet can in lowest order be understood on basis of Figure 1. As shown in the lower part of the figure, AF1 and AF2 generate potential wells and barriers for the accumulated charges. With the potentials on, holes are predominantly accumulated above AF2 and repelled from AF1. When the potentials on AF1 and AF2 are switched off, there is an excess of charges above AF2 that will spread by diffusion, and crucially for this device, by drift due to their mutual repulsion. When the potentials are switched on again, a fraction of the redistributed particles will get trapped in neighboring wells. Due to the asymmetry of the well/barrier pattern the fractions caught in the wells on the left and right of the initial well are typically unequal. Hence, upon repeated switching a net current results. This type of ratchet is commonly referred to as the on/off or flashing ratchet. It should be kept in mind that in general the highly non-linear behavior of ratchets cannot be understood from such a simplified picture.

We use the following notation for ratchets: an L*x*-*y*P*a* ratchet has *a* pairs of interdigitated fingers, with *a* ranging from 1 to 32 and a short and long spacing between the fingers AF1 and AF2 of *x* and *y* micrometer, respectively. Hence, an L1-4P8 ratchet has eight repetitions with a short and long spacing of 1 and 4 micrometer respectively. Since the width of the asymmetric fingers is 1 μm the repeat unit length $L = 7$ μm. In the simulations ratchets are infinitely periodic, hence they are denoted as L*x*-*y*P∞.

C. Ratchet efficiencies

The efficiency of ratchet systems is widely studied.[8–10] The commonly used definition for the efficiency of a Brownian motor connected to a load is:

$$\eta_p = \langle \dot{x} \rangle \, A_0 / \langle P \rangle_{in} \,, \tag{1}$$

with $\langle \dot{x} \rangle \, A_0$ the average mechanical work done per unit of time against an applied load A_0, and $\langle P \rangle_{in}$ the average net power pumped into the system. This same definition is used for the power efficiency of organic electronic ratchets:

$$\eta_p = \langle P_{out} \rangle \, / \, \langle P_{in} \rangle \tag{2}$$

The output power $\langle P_{out} \rangle$ is the time averaged (DC) source–drain current I_{SD} multiplied by the source–drain bias V_{SD}, normally taken at the maximum power point. The input power is the total amount of energy put into the system via the finger electrodes, averaged over one oscillation cycle $t = 2\pi/\omega$.

When no load is applied, the power efficiency is zero by definition. In order to make quantitative statements on how efficient a certain operation is performed under zero load, a generalized efficiency has been introduced for microscopic engines.[11] It is defined as $\eta = E_{\rm in}^{\rm min}/E_{\rm in}$, with $E_{\rm in}^{\rm min}$ the minimum energy input required to perform the same task as the engine, like moving through a viscous medium at constant temperature. Using this expression the operation of molecular motors in various situations can be compared.[11] For the same purpose, i.e. to compare electronic ratchets under zero load, the charge displacement efficiency η_q is introduced. In contrast to the just mentioned generalized efficiency, the charge displacement efficiency is not an energy-efficiency. It is defined as the net

amount of charge moved into one direction divided by the total amount of moved charge:[7]

$$\eta_q = \int I_{SD}(t)\,dt \Big/ \int |I_{SD}(t)|\,dt \tag{3}$$

where the integrals run over one oscillation cycle. In contrast to the generalized efficiency this is a measurable quantity, although practical realization of such a measurement is far from trivial.

A different number for how well these ratchets can move charges is the fraction of particles γ_t that is transferred from one asymmetric potential unit to a neighboring unit. It is found by dividing the net moved charge by the total amount of charge that is located in one asymmetric repeat unit. For a flashing ratchet γ_t can theoretically be as high as 16%.[10] It must be emphasized that γ_t is not the same as η_q. For the electronic ratchets discussed here the charge displacement efficiency η_q is a more meaningful number than the fraction of moved charges γ_t as it only takes into account those charges that participate in the charge transport and with that dissipate or deliver energy. In other words, static charges are not accounted for in η_q but are so in γ_t. Therefore γ_t is not further investigated. However, at the end of this paper, γ_t is calculated for an optimized ratchet and compared with the 16% found for the flashing ratchet.

D. Numerical model

The numerical model is identical to the one described in Ref. 7 and solves the coupled drift-diffusion and Poisson equations by forward integration in time. Since the smallest length scale in the devices is 1 μm, such a classical treatment is appropriate. For completeness, a brief description will be given here.

In the numerical modeling a single period of an infinitely long device is considered, as indicated by the dashed box in Figure 1. Hence, there are no contacts present and the source–drain bias V_{SD} is replaced with the tilt potential V_{tilt}, which is the applied potential over one asymmetric repeat unit. The model works on a 2D rectangular grid on which the device cross section is mapped. Apart from the tilt potential the left and right hand side of the calculation area are coupled via periodic boundary conditions, hence an infinitely long device is simulated. A zero vertical electric field is assumed for the top and bottom grid cell layers.

Transport of electrons and holes is described by the drift-diffusion, continuity and Poisson equations:

$$\begin{aligned} j^n &= q\mu_n n F + q D_n \nabla n \\ j^p &= q\mu_p p F - q D_p \nabla p \end{aligned} \tag{4}$$

$$\begin{aligned} q\frac{\partial n}{\partial t} &= \nabla j^n + q(G - R) \\ q\frac{\partial p}{\partial t} &= -\nabla j^p + q(G - R) \end{aligned} \tag{5}$$

$$\nabla \cdot (\varepsilon \nabla \phi) = q(n - p) \tag{6}$$

Here ϕ denotes the electrostatic potential, F the electric field, n and p are the free carrier concentrations of electrons and holes, and j^n and j^p are the electron and hole current density, respectively. D_n, D_p, μ_n and μ_p are the diffusion coefficients and the mobilities of electrons and holes, respectively. R and G are the recombination and (photo)generation rate, respectively. The generation rate is set to zero. $\varepsilon = \varepsilon_0 \varepsilon_r$ with ε_0 the permittivity of vacuum and ε_r the relative permittivity. As the devices studied here are hole-only and kept in the dark, n, R and G are all zero.

The Einstein relation between diffusion constant and mobility,

$$D_{n/p} = \frac{k_B T}{q}\mu_{n/p} \tag{7}$$

is assumed to hold. Here, k_B is the Boltzmann constant, T the temperature, and q the elementary charge.

For simplicity the gate and interdigitated fingers are collapsed on a single layer in the calculations. Moreover, the transport in the accumulation layer is assumed to be 1D.

Since charge transport in low mobility organic semiconductors occurs via hopping, phonon scattering is crucial but accounted for via the mobility.[12] Coulomb scattering from other particles or impurities is likely to yield only minor changes in the mobility.[13] Since the mobility is taken from experiment these effects are implicitly accounted for.

At time $t = 0$, a fixed amount of charge is placed inside the semiconducting layer. The amount of charge in the accumulation layer is calculated from the well-known formulas for a parallel plate capacitor in which the time-averaged gate potential at each grid point is used as the voltage applied over the capacitor plates. In subsequent small time steps, currents are calculated from Eq. (4), which, for each time step, give rise to a change in the carrier density according to Eq. (5) and to a new electrostatic potential according to Eq. (6). Steady state is reached when currents and carrier densities, averaged over one oscillation cycle, no longer change. Since displacement currents average out over a complete oscillation cycle they are not considered here.

III. RESULTS

In this section we systematically work our way towards electronic ratchet devices with an optimized performance in terms of charge displacement and power efficiencies. First, the current-voltage characteristics are discussed, after which the scaling of the performance with length scale, asymmetry and magnitude of the driving potential are investigated. These results are combined to optimize performance. We conclude this section with a brief discussion of the relations between the various efficiencies.

A. Output characteristics

In Figure 2(a), the modeled source–drain current I_{SD} is plotted versus the tilt potential V_{tilt} for different asymmetries. The frequencies f ($= \omega/2\pi$) used in the numerical modeling are the frequencies at which a maximum current value is reached ($f = f_I$). Figure 2(a) shows that for the infinitely long ratchets the simulations reveal a linear relationship between I_{SD} and V_{tilt}, in agreement with previously reported results.[8] The inset in Figure 2(a) shows the measured source–drain current versus source–drain bias for an L1–2P4 ratchet. The slight curvature in the experimental result is related to the presence of contacts.

Figure 2(b) displays the modeled average channel resistance R of one asymmetric period versus the repeat unit length L, which is the inverse slope of the I–V curves shown in Figure 2(a). Ratchets with constant (Lx–2xP∞ and Lx–4xP∞) and varying asymmetry (L0.5–yP∞) are modeled at $f = f_I$ and $f = f_Q$. The latter is the frequency at which the maximum charge per cycle is reached. The charge per cycle is the net amount of charges moved during one sequence and is obtained by dividing I_{SD} by the ratchet driving frequency f. At charge maximum, i.e. $f = f_Q$, a linear relationship is found between the channel resistance and length scale for different asymmetries, indicating that the asymmetry is not important for devices operating at f_Q. In another work it was already discussed that f_Q only depends on L and not on the asymmetry of the ratchet.[14] Also when comparing ratchets with a constant asymmetry operating at f_I, an (almost) linear dependence between the average channel resistance R and the repeat unit length L is found. For comparison, the lower solid line in Figure 2(b) shows the channel resistance without the ratchet mechanism turned on (i.e. V_A is set to 0 V in the model). An increase in channel resistance is observed when moving from 'ratchet off' to f_I to f_Q.

The data in Figures 2(a) and 2(b) can phenomenologically be described by the intersection point (V_0, I_L) of the I–V curves in panel (a) and by the channel resistance R, where R consists of a part that is linear in repeat unit length L and an almost constant offset term R_L. Unfortunately, the physical meaning of the parameters I_L and R_L is not very transparent. Clearly, they do represent a performance loss over an idealized device, but the associated power losses (≈70–95%) grossly underestimate the actual losses that will be discussed below. Nevertheless, the fact that I_L and R_L are

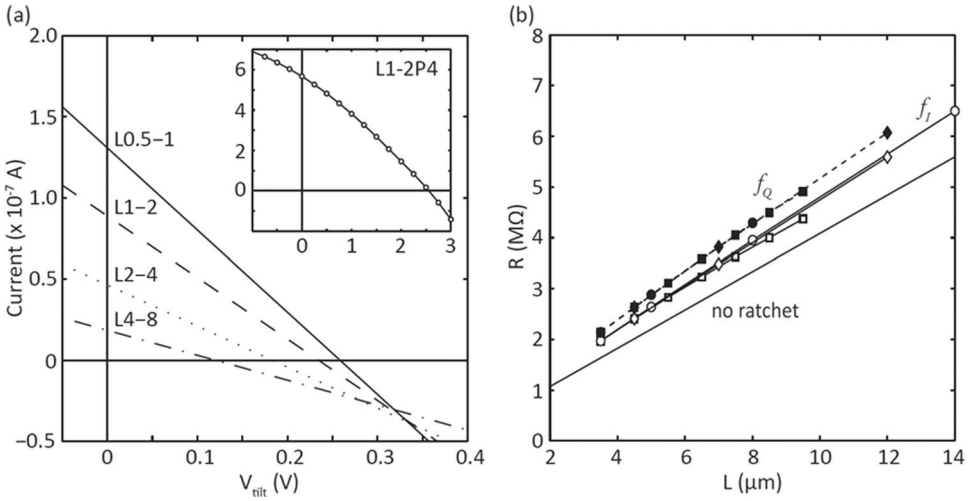

FIG. 2. (a) Modeled current I_{SD} versus tilt potential V_{tilt} for several Ly–2yP∞ ratchets (constant asymmetry, L0.5–1P∞, L1–2P∞, L2–4P∞, and L1–4P∞) at f_I. The inset shows a measurement result of the current versus source–drain bias V_{SD} for an L1–2P4 ratchet. (b) Modeled channel resistance R versus characteristic length L for ratchets with constant (Ly–2yP∞, Ly–4yP∞) and varying (L0.5–yP∞) asymmetry at f_I and f_Q. The solid line shows the channel resistance for a structure where the ratchet is turned off (i.e. $V_A = 0$ V). Modeling settings are: $\mu = 10^{-6}$ m^2/Vs, $V_G = -20$ V, $V_A = 8$ V, $V_O = -7$ V, $= 180°$ and $V_{SD} = 0$ V. For the Ly–2yP∞ series, $y = 0.5$, 1, 2, and 4 (only f_I). For the Ly–4yP∞ series, $y = 0.5$, 1, and 2. For the L0.5–yP∞ series, y ranges from 1 to 7.

nonzero shows that the system can only in crude approximation be treated as a linear superposition of an ideal charge pump (the ratchet) and an internal load (the channel resistance). On the other hand, given the highly non–linear nature of ratchets in general, the relatively small values of I_L and R_L may be considered surprising.

The open circuit voltage remains constant when the mobility is changed, just like the charge per cycle (not shown). This is a direct consequence of the fact that the mobility sets the time scale at which carrier motion takes place, but has no effect when the other time scales in the system -in this case the driving frequency f- are scaled accordingly.[10,14] Another consequence of this scaling of time scales with mobility is that the charge per cycle versus frequency curve $Q(f)$ shifts linearly with mobility, but doesn't change shape or height. In Ref. 7 it was already shown that $f_I \sim \mu$. Hence, the current $I_{SD} = Q(f)f$ scales linearly with mobility. Modeling results (not shown) confirm that indeed $I_{SD} \sim \mu$.[8,15]

B. Scaling with length

The charge displacement efficiency and power efficiency at f_I (solid lines) and f_Q (dashed lines) versus L^{-1} corresponding to the devices in Figure 2 (and S1) are displayed in Figure 3(a) and 3(b). For ratchets with constant asymmetry, the charge displacement (c) and power efficiencies (d) at f_I show a small increase for increasing L. When looking at ratchets with varying asymmetry (L0.5–yP∞) a maximum in charge displacement efficiency is reached for the L0.5–5P∞ ratchet and in power efficiency for the L0.5–4P∞ ratchet. The charge displacement and power efficiencies for ratchets operating at f_Q are larger than those at f_I and show a sharper increase with increasing repeat unit length. These particular devices show respectable efficiencies as charge pumps, i.e. 3 to 17% of all charge motion is directed for the used settings. Unfortunately, the associated power efficiencies lay below 0.5%. The relation between charge displacement and power efficiency will be discussed below. At the end of this paper it will be shown that in particular the power efficiency can be significantly enhanced.

The data in Figure 3 show in general an increase in current for smaller ratchets at the cost of a decrease in the charge displacement and power efficiencies. In order to achieve higher currents without losing efficiency the mobility should therefore be increased, which comes at the cost of an

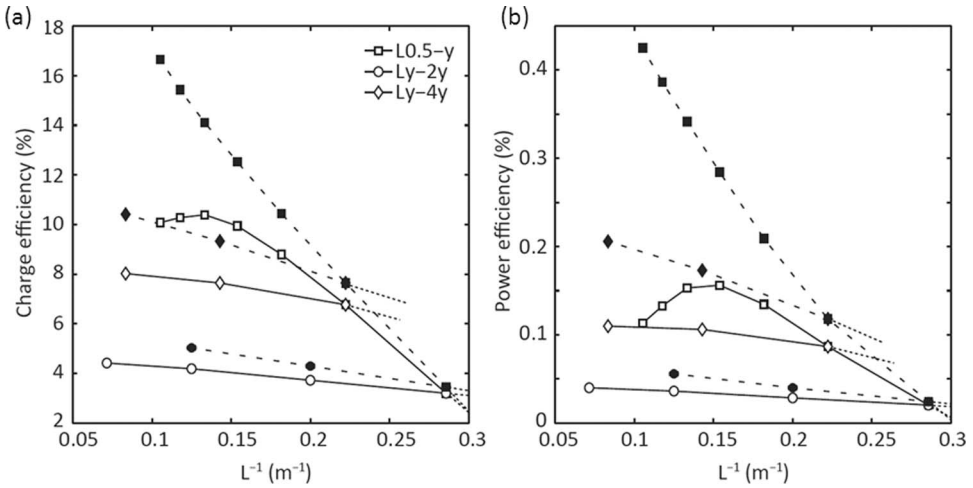

FIG. 3. Calculated charge displacement efficiency η_Q (a) and power efficiency η_P (b) versus L^{-1} for ratchets with constant (Lx–2xP∞, Lx–4xP∞) and varying asymmetry (L0.5–yP∞) at f_I (solid lines) and f_Q (dashed lines). Modeling settings are: $\mu = 10^{-6}$ m^2/Vs, $V_G = -20$ V, $V_A = 8$ V, $V_O = -7$ V, $\varphi = 180°$ and $V_{SD} = 0$ V. Corresponding short-circuit currents and open-circuit voltages are shown in Figure S1 in the supplemental material.[16]

increased operating frequency. In practice this requires the use of higher mobility materials than the pentacene used here. This scaling relies, as discussed above, on the fact that the charge per cycle versus frequency curve only shifts with mobility without changing shape. Implicitly, we have also made use of the fact that the frequency at which the charge per cycle maximum is reached is almost equal to the frequency at the maximum in charge displacement efficiency.

C. Influence of driving potential magnitude

The influence of the amplitude V_A and the offset V_O of the driving potential on the current is investigated in Figure 4, where a calculated current contour plot for an L1–4P∞ ratchet (a) is compared to the same plot as measured for an L1–4P2 ratchet (b). As the frequency is kept constant in these plots, the current contour plots also resemble the shape of the charge per cycle contour plots. The modeled and measured plots are very similar in shape. For both plots, no (change in) current is observed for $V_O \geq V_{TH}$ with V_{TH} the transistor threshold voltage. In this offset region (denoted I), DC currents are blocked since the accumulation layer is locally depleted –the applied potential on AF1 is continuously higher than the threshold voltage. For the model the threshold voltage is 0 V.

The region of significant current transport (II) has a triangular shape, and is enclosed by the lines $V_O = V_{TH}$ and $V_A = |V_O - V_{TH}|$. In region (II) the potential on the asymmetric finger electrodes AF1 exceeds the threshold voltage for a fraction of each oscillation period, which drastically increases the current for unknown reasons. Naively, one could imagine that a temporary blocking of the channel by one set of fingers improves the pumping action of the other, but the simulations show that the channel does not, at any moment during the oscillation cycle, get depleted. The panels in Figure 4 are typical results. As a rule of thumb the optimum offset–amplitude ratio for current transport for these ratchets is 1:2, indicated by the dashed–dotted lines.

In region (III) (where $V_A \leq |V_O - V_{TH}|$) the current transport seems negligible. However, in this region the non–linear behavior of these ratchets becomes clear once more. When in this region the current is plotted as a function of amplitude at constant offset, current reversals rather than a monotonous increase appear as shown in Figure S2. The modeled current changes linearly with the amplitude in region II (Figure S2). These current reversals cannot be seen in the measured current contour plots due to the used amplitude step size (0.5 V) and the low current values which are in the order of the background noise.

The dashed line in region II of Figure 4 indicates that maximum output is reached when -in a quasi-static view- AF1 depletes the channel half the time. Since the finger electrodes are embedded

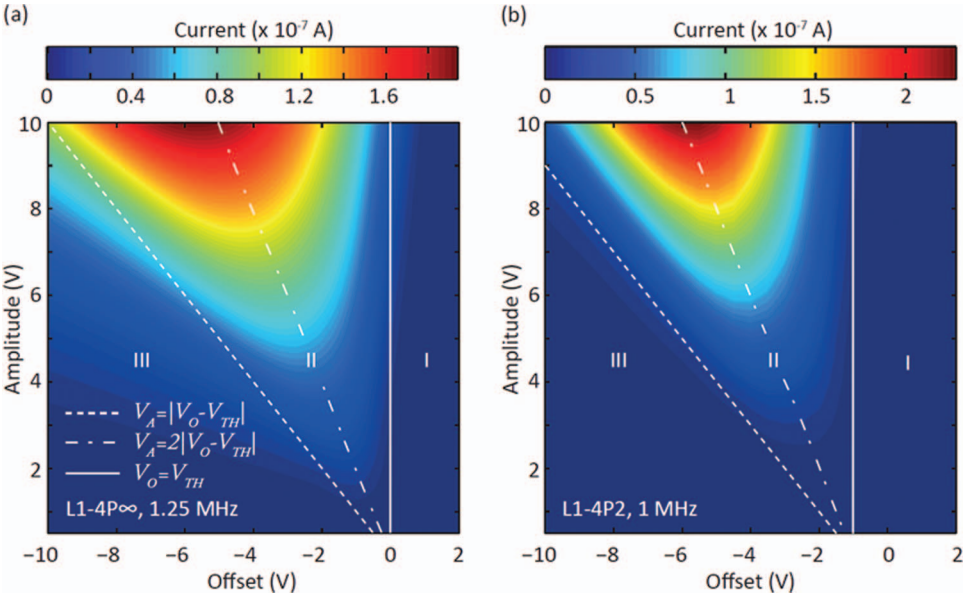

FIG. 4. Contour plot of current as a function of the applied amplitude V_A and offset V_O for a modeled L1–4P∞ ratchet (a) and a measured L1–4P2 ratchet (b). Modeling settings for (a) are: $\mu = 10^{-6}$ m^2/Vs, $V_G = -20$ V, $f = 1.25$ MHz, $= 180°$, and $V_{SD} = 0$ V. Measurement settings for (b) are: $V_G - V_{TH} = -20$ V, $f = 1$ MHz, $= 180°$, and $V_{SD} = 0$ V.

in the gate dielectric, the depletion is independent of the bias on the lower lying gate. It appears from simulations and measurements (not shown) that maximum charge efficiency is reached for gate voltages that are a few V below the threshold voltage.

D. Optimized efficiency

So far, the influence of length scale L, mobility μ, amplitude V_A, offset V_O, on the current transport and on the charge displacement and power efficiencies were investigated and, where possible, rationalized. In this section all results are combined to optimize the efficiency of the ratchets. An L1–8P∞ ratchet is chosen since the 1:8 ratio gives the optimal power efficiency, as shown in Figure 3(d). A realistic amplitude of 10 V is chosen with, according to the rule of thumb introduced in the discussion of Figure 4, a matching offset of –5 V and a gate voltage of –4 V. In Figure 5, contour plots of the charge per cycle (a) and charge displacement efficiency (b) are shown as a function of frequency and phase angle between AF1 and AF2.

When the phase is varied between 0° and 360° two current reversals occur as anticipated. However, the efficiency minimum is smaller in magnitude than the maximum and occurs at a lower frequency. Also the phase difference between the efficiency minimum and maximum is approximately but not exactly 180°. These effects are direct consequences of the fact that changing the phase by 180° does not completely invert the potential; this requires the additional transformation $V_A \rightarrow -V_A$. This behavior is also visible in the device current; see Figure S2 in which measured and calculated currents are plotted versus phase and frequency.

For the chosen parameters a charge displacement efficiency η_q in excess of 49% is obtained. The maximum power efficiency when a load is applied to the ratchet is calculated to be as large as 6.9%. Interestingly, these high efficiencies occur at frequencies of O(10^4) Hz where both drift and diffusion are significant, and which are far below f_I, i.e. the frequency of O(10^6) Hz where the maximum output current is reached.[7] Since the highest efficiencies are found at the lowest frequencies used in the calculations, the present numbers should be regarded as lower limits. Unfortunately, calculation times become prohibitively long at even lower frequencies.

The importance of diffusion at low frequencies makes the temperature dependence of the ratchet performance potentially interesting and this will be subject of further study. At frequencies around

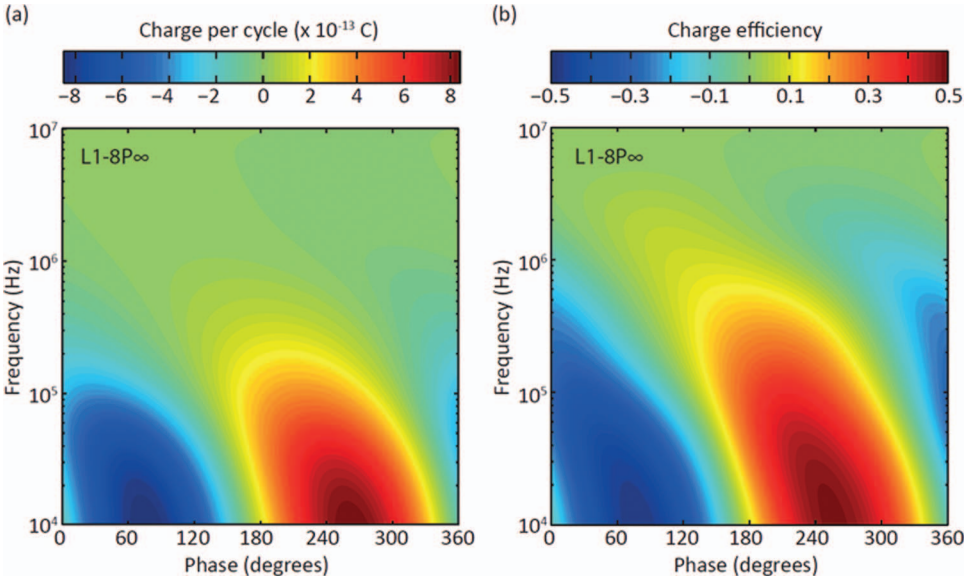

FIG. 5. Calculated contour plots of charge per cycle (a) and charge displacement efficiency η_Q (b) as a function of frequency f and phase φ for an L1–8P∞ ratchet. Modeling settings are: $\mu = 10^{-6}$ m^2/Vs, $V_G = -4$ V, $V_A = 10$ V, $V_O = -5$ V, and $V_{SD} = 0$ V.

maximum output the device is drift-dominated, and the temperature dependence will reduce to a scaling of the mobility.[7,14]

E. Relation between different efficiencies

When all parameters are optimized and the charge displacement efficiency at $V_{tilt} = 0$ V is known, the power efficiency can be estimated quite accurately. The power efficiency is defined as $\eta_p = \langle P_{out}\rangle/\langle P_{in}\rangle$, which equals $\eta_p = I_{DC}^2 R/\langle I_{AC}^2 R'\rangle$. The latter term $\langle I_{AC}^2 R'\rangle$ consists of local time–varying currents I_{AC} and local time–varying resistances R', integrated over space and time. The current I_{DC} is the current at the maximum power point. For the infinitely long ratchets that are modeled this is half the current at short circuit (Figure S1a). Substituting I=$Q/\Delta t$, the power efficiency becomes $\eta_p = Q_{SC}^2 R/4\langle Q_{AC}^2 R'\rangle$.

When it is assumed that the channel resistance is constant and homogeneously distributed over the channel, $R' = R$ one finally arrives at the simple expression $\eta_p = Q_{SC}^2/4\langle Q_{AC}^2\rangle = \eta_q^2/4$. This back–of–the–envelope estimation turns out to be correct within a factor 2 for the modeling results of the charge displacement and power efficiencies shown in Figure 3. However, when all parameters -i.e. V_G, V_A, V_O, f, - are optimized the estimate is correct within a few percent.

The fraction of moved particles γ_t, defined in section II C, is calculated at about 11% for this optimized ratchet. There is a large gap with the charge displacement efficiency of 49% which indicates that a large fraction of charges does not participate in the charge transport. Nevertheless, there is only a 5 percentage points difference with the theoretical upper limit of 16% estimated for the flashing ratchet.[10] The latter value is an estimate for the fraction of non–interacting particles that per cycle is moved to the next-nearest well in an optimized device. Also because the organic electronic ratchets are operated in a quasi–flashing mode, a sinusoidal rather than a square wave potential is applied to the finger electrodes, the 16% value should not be regarded as a formal upper limit. In either case, it goes to show that ratchets can displace charge carriers with significant efficiency.

IV. CONCLUSION

In summary, the performance of electronic ratchets is investigated by numerical modeling and measurements. It is shown how the characteristic parameters of the time–varying asymmetric

potential like length scales and amplitude, as well as the charge carrier density and mobility influence the performance. For ratchets with a constant asymmetry but changing length, the current increases when going to smaller length scales but the net charge displaced per cycle, as well as the power and charge displacement efficiencies decrease. Similarly, the highest efficiencies are found at frequencies far below those where the maximum current is obtained: to optimize the power efficiency for a given geometry, settings need to be chosen such that the charge displaced per oscillation cycle reaches a maximum, rather than near the current maximum. Hence, to increase the current while preserving power efficiency, the mobility of the semiconductor must be increased –note that the presented results are not specific for the (organic) semiconductor used. Accordingly, the operating frequency must be increased proportionally. When all settings are brought close to optimum a ratchet with a charge displacement efficiency of over 49% is found and with a power efficiency of approximately 6.9%. These numbers show that properly controlled ratchet potentials can rectify external perturbations with considerable efficiency.

[1] Smoluchowski, M. v., Experimentell Nachweisbare, der Üblichen Thermodynamik Widersprechende Molekularphänomene (Eng.: 'Experimentally confirmed, molecular phenomena opposing the conventional thermodynamics'), Physikalische Zeitschrift **13**, 12 (1912).
[2] Feynman, R. P., Sands, M. L. & Leighton, R. B., *The Feynman lectures on physics* (Addison-Wesley, 1989).
[3] van Oudenaarden, A. & Boxer, S. G., Brownian ratchets: Molecular separations in lipid bilayers supported on patterned arrays, Science **285**, 1046-1048 (1999); J. Rousselet, L. Salome, A. Ajdari & J. Prostt., Directional motion of brownian particles induced by a periodic asymmetric potential, Nature **370**, 446-447 (1994).
[4] Linke, H. *et al.*, Experimental tunneling ratchets, Science **286**, 2314-2317 (1999).
[5] Khrapai, V. S., Ludwig, S., Kotthaus, J. P., Tranitz, H. P. & Wegscheider, W., Double-dot quantum ratchet driven by an independently biased quantum point contact, Phys. Rev. Lett. **97**, 176803 (2006).
[6] Fujiwara, A., Nishiguchi, K., Ono, Y., Nanoampere charge pump by single-electron ratchet using silicon nanowire metal-oxide-semiconductor field-effect transistor, Appl. Phys. Lett. **92**, 042102 (2008).
[7] Roeling, E. M. *et al.*, Organic electronic ratchets doing work, Nat Mater **10**, 51–55 (2011).
[8] Reimann, P., Brownian motors: noisy transport far from equilibrium, Physics Reports–Review Section of Physics Letters **361**, 57–265 (2002).
[9] Hänggi, P. & Marchesoni, F., Artificial Brownian motors: Controlling transport on the nanoscale, Rev Mod Phys **81**, 387–442 (2009).
[10] Linke, H., Downton, M. T. & Zuckermann, M. J., Performance characteristics of Brownian motors, Chaos **15**, 026111 (2005).
[11] Derenyi, I., Bier, M. & Astumian, R. D., Generalized efficiency and its application to microscopic engines, Phys Rev Lett **83**, 903–906 (1999).
[12] Coehoorn, R., Pasveer, W. F., Bobbert, P. A. & Michels, M. A. J., Charge-carrier concentration dependence of the hopping mobility in organic materials with Gaussian disorder, Phys. Rev. B. **72**, 155206 (2005).
[13] Sharma, A., Janssen, N. M. A., Mathijssen, S. G. J., de Leeuw, D. M., Kemerink, M. & Bobbert, P. A., Effect of Coulomb scattering from trapped charges on the mobility in an organic field-effect transistor, Phys. Rev. B **83**, 125310 (2011).
[14] Roeling, E. M. *et al.*, Scaling of characteristic frequencies of organic electronic ratchets, Unpublished.
[15] Scheinert, S. & Paasch, G., Fabrication and analysis of polymer field–effect transistors, Phys Status Solidi A **201**, 1263–1301 (2004).
[16] See supplementary material at http://dx.doi.org/10.1063/1.3677934 for device current vs drive amplitude and device current vs. phase and frequency of driving potential are discussed. This material is available free of charge via the Internet.